Virtual energy storage system for voltage control of distribution networks

Saif Sabah Sami, *Member, IEEE*, Meng Cheng, Jianzhong Wu, *Member, IEEE* and Nick Jenkins, *Fellow, IEEE*[*]

***Abstract*—Increasing amount of Distributed Generation (DG) connected to distribution networks may lead to the voltage and thermal limits violation. This paper proposes a Virtual Energy Storage System (VESS) to provide voltage control in distribution networks in order to accommodate more DG. A VESS control scheme coordinating the demand response and the energy storage system was developed. The demand response control measures the voltage of the connected bus and changes the power consumption of the demand to eliminate voltage violations. The response of energy storage systems was used to compensate for the uncertainty of demand response. The voltage control of energy storage system is a droop control with droop gain values determined by voltage sensitivity factors. The control strategy of the VESS was applied to a medium-voltage network and results show that the control of VESS not only facilitates the accommodation of higher DG capacity in the distribution network without voltage violations or network reinforcements but also prolongs the lifetime of transformer on-load tap changer.**

***Index Terms*— Virtual energy storage system, demand response, energy storage system, distributed generation, distribution network, voltage control.**

I. Introduction

MODERN distribution networks are witnessing significant challenges to control the network voltage due to changes in generation mix and demand. Decarbonisation of heat and transport sectors supported by the growing number of electric heat pumps and electric vehicles may cause under-voltage problems. In contrast, the connection of Distributed Generation (DG) may create over-voltage problems. In the Great Britain (GB) power system, only 18 % of DG are fully visible to the system operator at present [1]. Around 40% of the renewable energy generation in GB is connected to distribution networks [2]. That can pose a serious threat to the distribution network voltage management, which results in a slow progress of integrating DG into the distribution network.

Several studies have been conducted to investigate the use of energy storage systems, switched capacitors and DG active and reactive powers for the distribution network voltage control [3]. A single 6 MW/10 MWh batteries energy storage system was installed in a distribution network to defer the substation upgrade of adding a third 38 MVA transformer and to provide voltage support [4]. In [5], a centralised coordinated voltage controller of multiple batteries energy storage system and transformers with On-Load Tap Changer (OLTC) was proposed to solve over-voltage and voltage unbalance problems caused by DG in the distribution network. The proposed method does not involve a coordination among batteries energy storage system units. Instead, a coordinated control of multiple batteries energy storage system for voltage control of low-voltage networks is presented in [6]. The coordinated centralised controller determines which batteries energy storage system will be used to solve voltage problems based on all units' state of charge and voltage sensitivity factors.

However, costs remain the main barrier to the large-scale deployment of energy storage system, in addition to the costs of the Information and Communication Technologies (ICT) infrastructure for the central controller implementation.

It is estimated in [7] that demand response has the potential to reduce the energy storage system market size by 50% in 2030. In [8], the peak reduction from flexible commercial and industrial loads is forecasted to be approximately 10% of the GB power system peak load in 2030. In recent years, several studies were undertaken [9] investigating demand response abilities to provide ancillary services to the power system. These services include voltage control of the distribution network. In [10], a centralised control scheme was proposed. The control monitors the bus voltage through Remote Terminal Units (RTU) and determines the required load curtailment of the customers participating in a distribution network program based on voltage sensitivity factors. However, the challenges facing distribution network are the uncertainty of the response and the consequent reduction in the diversity among these flexible loads after the provision of the response.

Several studies proposed a centralised coordinated control of demand response and battery energy storage system units to minimises electricity costs in buildings [11] and to reduce operational costs and embedded diesel generation emissions in Microgrids [12]. In [13], a centralised coordinated control

[*] The work was supported in part by Higher Committee for Education Development in Iraq (HCED), by RESTORES project under the grant (No. EP/L 014351/1) of UK-EPSRC, by JUICE project under the grant (No. EP/P003605/1) and by P2P-SmarTest project under the grant of EU commission.

All authors are with the Institute of Energy, School of Engineering, Cardiff University, Cardiff CF24 3AA, UK (E-mail addresses: SamiSS@cardiff.ac.uk (S.S. Sami), Chengm2@cardiff.ac.uk (M. Cheng), WuJ5@cardiff.ac.uk (J. Wu), JenkinsN6@cardiff.ac.uk) (N. Jenkins).

algorithm of demand response and battery energy storage system was presented for tie-line smoothing of a Microgrid with integrated DG Results illustrate that coordinating with demand response can significantly reduce the required size of energy storage system [13].

A Virtual Energy Storage System (VESS) consisting of demand response and an energy storage system was developed to support the distribution network voltage and hence allows more DG integration in the distribution network. The VESS concept and its potential applications are first introduced. Then, modelling and control of VESS components and VESS control scheme are presented. A population of industrial Bitumen Tank (BT) and battery energy storage system were used to demonstrate the performance of the proposed voltage control scheme of the VESS. Two types of DG, solar and wind generation, and the VESS are connected to a Medium-Voltage (MV) network of the United Kingdom generic distribution system (UKGDS). The VESS control scheme operates cooperatively with on-load tap changers to ensure that no voltage hunting will take place. The proposed VESS control was evaluated by time series analysis through different seasons of a year.

II. VESS Concept and Potential Applications

A. VESS Concept

A VESS aggregates miscellaneous controllable components of an energy systems to form a single entity, which can behave similarly to a large capacity energy storage system with reduced capital costs. Examples of such components include flexible loads with thermal storage such as electric heaters, DG such as Combined Heat and Power units (CHP) or conventional energy storage systems. The VESS allows those components to access to the electricity and ancillary markets in order to provide transmission and/or distribution level services.

B. Potential Applications

By aggregating different types of energy resources, the VESS can be characterised as a high-power and high-energy density energy storage system. Hence, its potential applications extend over a widespread multi-disciplines of the power system [14]. These include but not limited to, providing energy arbitrage, facilitating renewable integration in distribution network, deferring the transmission and distribution systems reinforcements and providing ancillary services such as frequency response, voltage support and power quality improvements.

III. Modelling of VESS Components

A. Model of Demand Response Units

A thermodynamic model depicting variations of the temperature of industrial Bitumen Tanks (BT) with time was developed based on [15]. BT heat supply power P_{supply} (W), its heat loss power P_{loss} (W) and its net heat transfer power P_{net} (W) are:

$$P_{supply} = P \times S_{final} \quad (1)$$

$$P_{loss} = U \times A \times (T - T_{amb}) \quad (2)$$

$$P_{net} = P_{supply} - P_{loss} \quad (3)$$

where P (W) is the power consumption of the heater, S_{final} is the heater state (S_{final} = 1 if heater is ON and S_{final} = 0 if heater is OFF), U $(Wm^{-2}\cdot{}^oC^{-1})$ is the overall heat transfer coefficient, A (m^2) is the area of the tank surface, T (^oC) is the internal temperature of the tank and T_{amb} (^oC) is the ambient temperature.

The heat transfer inside a tank leads to a temperature change dT (^oC). The internal temperature change can be associated with the net heat transfer as

$$P_{net} = c_v \times m \times \frac{dT}{dt} \quad (4)$$

where c_v $(Jkg^{-1}\cdot{}^oC^{-1})$ is the specific heat capacity of the tank and m (kg) is the mass. Combining (1)-(4), the tank internal temperature variations are depicted by a first-order differential equation (5)

$$\frac{dT}{dt} = \frac{P \times S_{final}}{c_v \times m} - \frac{U \times A \times (T - T_{amb})}{c_v \times m} \quad (5)$$

The general solution of (5), which is the variations of temperature over time, can be depicted by exponential functions depending on the state of S_{final}. It is required that the tank internal temperature be maintained all the time between its low set-point (T_{low}, typically 150º) and its high set-point (T_{high}, typically 180º). Therefore, the BT thermodynamic model was developed using (6)-(7):

$$S_{final}=1:\ T_{(t)} = 184.68 - 34.68 \times e^{-\frac{t}{\tau_{ON}}} \quad (6)$$

$$S_{final}=0:\ T_{(t)} = 145.32 + 34.68 \times e^{-\frac{(t-t_{ON})}{\tau_{OFF}}} \quad (7)$$

where τ_{ON} and τ_{OFF} are the time constants which were obtained through field measurements to be half of the ON and OFF periods (t_{ON} and t_{OFF}) of each BT [16]. According to the field tests in [15], for a population of BTs, the ON-period and OFF-period were randomly distributed within the range of 30 min to 360 min and of 60 min to 1140 min.

B. Model of Energy Storage System

A simplified model of batteries energy storage system model was developed in [17], which consists of a generic battery model and a simplified power electronics model. The generic battery model ('Module (Battery cells)' in Fig. 1 is composed of a controllable voltage source, a controllable current source and a resistance connected in series. The charging and discharging characteristics are assumed similar. The simplified power electronic converters model is a first-order lag to represent the delays in the converters control loop.

In this study, Lithium-Ion batteries were modelled. A (DC/AC) Voltage Source Converter (VSC) was assumed to connect the batteries to the distribution network. Hence, the active and reactive power are controlled independently and only the active power passes to the batteries and therefore affects the stored energy in the batteries energy storage system. The reactive power is supplied by the converter. Furthermore, the power converter internal losses were neglected and a 90% roundtrip efficiency of batteries energy storage system was considered.

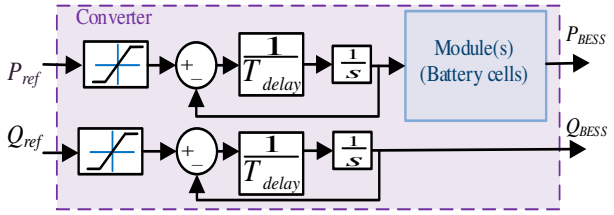

Fig. 1. Simplified batteries energy storage system model.

IV. Voltage Control of VESS

A. Voltage Control of Demand Response Units

A distributed voltage controller was added to each Bitumen Tank inherent temperature control. The voltage controller alters demand response units' power consumption based on local voltage measurements as shown in Fig. 2. The temperature control measures the temperature T of a tank and generates state signals S_T. The voltage control measures the bus voltage V and generates state signal S_{HV} and S_{LV}. The final switching signal S_{final} to the heater is then determined by logic gates, which ensures the priority of the temperature control. Therefore, the extra voltage control will not undermine the hot storage function of BTs.

The voltage control algorithm switches on/off the load in response to voltage deviations. The control algorithm assigns a pair of voltage set-points, namely V_{ON} and V_{OFF}, which dynamically and linearly varies with the temperature of a BT. For example, a BT will have a higher V_{ON} and lower V_{OFF} values if its temperature is higher than other BT temperature. The control algorithm continuously compares the measured voltage (V) with the set-points. If voltage V is higher than V_{ON}, the voltage control generates a state signal S_{HV} and the load is switched on. In contrast, if voltage V is lower than V_{OFF}, the voltage control generates a state signal S_{LV} and the load is switched off. The linear variation of V_{ON} and V_{OFF} with temperature ensures that among a population of BTs, following a voltage drop, the BT with the highest temperature will be switched off first because it is most willing to be switched off because its temperature has already been high. On the contrary, BTs will be switched on in response to a voltage rise starting from the BT with the lowest temperature. Therefore, the number of BTs committed to respond to voltage deviations increases linearly with the increase in voltage deviations. Hence, all the demand response units are committed if the voltage accessed the limits. It was assumed that the distribution network voltage limits follow the British Standard EN 50160 [18], a distribution network with voltage limits of ± 6% of nominal value (i.e. 0.94 p.u.-1.06 p.u.), and voltage control dead-band of ± 3% (i.e. 0.97 p.u.-1.03 p.u.) were used. BTs have low and high temperature limits of 150ºC and 180ºC.

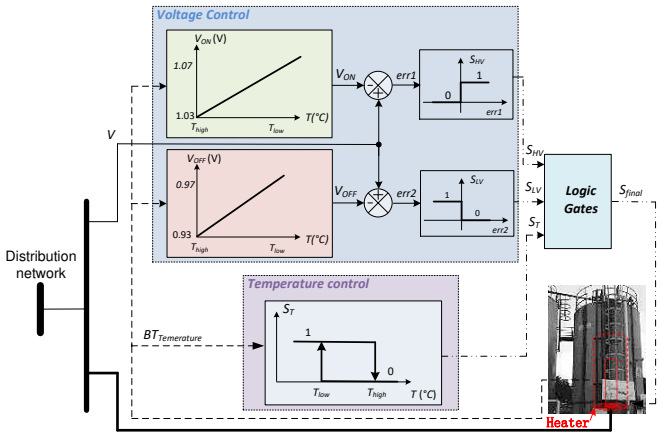

Fig. 2. The control system of a flexible load

B. Voltage Control of Energy Storage System

Energy Storage System (ESS) control methodology consists of a main and a supplementary controllers. The main controller drives ESS's active and reactive power output in response to voltage violations. The supplementary controller maintains ESS's state of charge value within a certain range, which facilitates a secure, sustainable and efficient operation.

Energy storage system active and reactive power outputs are determined by a droop control and the droop setting is obtained based on voltage sensitivity factors matrices.

1) Voltage Sensitivity Factors Matrices

Voltage sensitivity factors relate the change in voltage at a bus to a change in active and/or reactive power(s) at other buses in the network [19]. In a voltage sensitivity factors matrix, a high voltage sensitivity factors implies that a change in active and reactive power at a bus drives a large change in voltage at the corresponding bus.

Voltage sensitivity factors matrices (10)-(11) were extracted from the Jacobian matrix in (8)

$$\begin{bmatrix}\Delta P\\ \Delta Q\end{bmatrix}=\begin{bmatrix}\frac{\partial P}{\partial \delta} & \frac{\partial P}{\partial V}\\ \frac{\partial Q}{\partial \delta} & \frac{\partial Q}{\partial V}\end{bmatrix}\begin{bmatrix}\Delta \delta\\ \Delta V\end{bmatrix} \tag{8}$$

$$\Delta V = M\cdot\Delta P + N\cdot\Delta Q \tag{9}$$

where

$$M=\left[\frac{\partial P}{\partial V}-\frac{\partial P}{\partial \delta}\cdot\left[\frac{\partial Q}{\partial \delta}\right]^{-1}\cdot\frac{\partial Q}{\partial V}\right]^{-1} \tag{10}$$

$$N=-M\cdot\frac{\partial P}{\partial \delta}\cdot\left[\frac{\partial Q}{\partial \delta}\right]^{-1} \tag{11}$$

2) Droop Control of Energy Storage System Using Voltage Sensitivity Factors

A brief network analysis was carried out to identify the most vulnerable buses with respect to voltage violations. These buses are often the ones loaded heavily, connected to large DG or connected through small capacity branches. Then, these buses are equipped with remote monitoring devices to monitor and to send voltage values to the ESS controller.

The ESS controller receives the voltages of the buses and classifies the voltages into zones based on British Standard EN 50160 [18] as illustrated in Fig. 3 to the following:

1. Red zones (RH and RL) represent the voltage violation ranges, i.e. bus voltage violates/exceeds the ± 6% limits.
2. Yellow zones (YL and YH) represent the severe voltage deviation ranges, i.e. bus voltage largely deviates (equal or

larger than ± 3%) from the nominal value yet within the limits.

3. Green zones (GL and GH) represent the slight voltage deviation ranges, i.e. bus voltage marginally deviates (smaller than ± 3%) from the nominal value.

In the worst case, the network will suffer from high voltage deviations in both high and low voltage directions (i.e. two directions). To address this case, two buses with two largest voltage deviations are selected and placed on the vertical and horizontal axes of Table I. In case of having more than two monitored buses with voltage violations, it is assumed that by mitigating the extremes cases, the less severe voltage violations will also be released. One of these buses is considered as the designated bus. Following rules will be applied to determine the designated bus and the charging/discharging actions:

- If both buses (in Table I) have a similar direction of voltage diversions (i.e. both bus voltages are above/below the nominal value), the designated bus is the bus with the largest voltage violation (RH or RL). ESS responds with enough power to bring the designated bus voltage back within the limits (cells 1,2,3,12,14, and 15 in Table I).
- If the two buses have opposite direction of voltage violations. ESS takes no action (cell 5 in Table I).
- If the two buses have opposite direction of voltage deviation (i.e. one bus voltage is above the nominal value and the other is below), the designated bus is the none voltage violation bus (YL or YH). ESS responds with enough power to push designated bus's voltage deviation to the limits, therefore reduce the other bus voltage violation (cells 4 and 9 in Table I).
- If no voltage violation occurs, i.e. all monitored bus voltages are within limits. ESS takes no action (cells 6,7,8,10,11, and 13 in Table I).

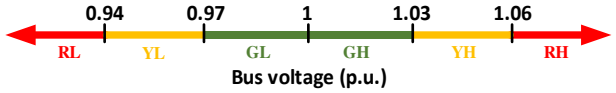

Fig 3: Classified bus voltage zones

ESS will response by a droop control with respect to the designated bus *i*. The required voltage change at the designated bus *i* (ΔV_i in p.u.) is determined first to calculate the required changes of active power (ΔP_{ES} in p.u.) and reactive power (ΔQ_{ES} in p.u) from ESS by using (12).

$$\Delta V_i = M_{i\,ESS} \times \Delta P_{ESS} + N_{i\,ESS} \times \Delta Q_{ESS} \quad (12)$$

$M_{i\,ESS}$ is the voltage sensitivity factor relating the change in the ESS active power to the change in bus *i* voltage and $N_{i\,ESS}$ is the voltage sensitivity factor relating the change in ESS reactive power to the change in bus *i* voltage.

TABLE I
ENERGY STORAGE SYSTEM VOLTAGE CONTROL SETTINGS

	RH	YH	G	YL	RL
RH	1 C_{RH}				
YH	2 C_{RH}	6 0			
G	3 C_{RH}	7 0	10 0		
YL	4 C_{YL}	8 0	11 0	13 0	
RL	5 0	9 D_{YH}	12 D_{RL}	14 D_{RL}	15 D_{RL}

where:

C_{RH}: Charge ESS with respect to the bus with highest voltage violation

D_{RL}: Discharge ESS with respect to the bus with lowest voltage violation

C_{YL}: Charge ESS with respect to the bus with lowest voltage deviation

D_{YH}: Discharge ESS respect to the bus with highest voltage deviation

0 : No ESS power output

The ESS reactive power response is prioritised above its active power response in order to minimise the charging and discharging of the battery. The required reactive power can be obtained by setting the active power to zero in (12). Alternatively, if the required reactive power is higher than its rated value, the ESS will provide both active and reactive power. The required active power can be obtained by setting the reactive power to its rated value in (12).

3) Supplementary Control of Energy Storage System

When all monitored bus voltages are in the green zones (Fig. 3), the ESS supplementary control restores the state of charge to 50±10%. The ESS charges/discharges using droop control with respect to the monitored bus with the highest voltage sensitivity factors. The ESS responds with enough power to push this bus voltage to the yellow zone (Fig. 3). This ensures that consuming/absorbing ESS power will not cause voltage violations. Only the active power of (12) is used and the reactive power is set to zero. Consequently, any forthcoming charging or discharging requirements are expected to be met.

C. Coordinated Voltage Control of VESS

The coordination between demand response and energy storage system in the VESS is achieved by setting their controllers with different time delay constraints. As a result, they will not conflict with each other and cause voltage hunting. The time delay constant coordination also considers conventional voltage control equipment including the OLTC and Voltage Regulators (VR). When a voltage violation occurs, the voltage controllers of Demand Response (DR) units respond first with a time delay constant τ_{DR}. If the voltage violation continues, the Energy Storage System (ESS) with a time delay constant τ_{ESS} (i.e. $\tau_{ESS} > \tau_{DR}$) will respond secondly. This procedure ensures that no voltage violation will take place due to the uncertainty of demand response. Then if required, On-Load Tap Changer (OLTC) will take action lastly with a time delay constant τ_{OLTC} (i.e. $\tau_{OLTC} > \tau_{ESS}$). This, in turn, results in less OLTC actions.

V. Test System

In this paper, the performance of the proposed VESS voltage control scheme was evaluated using a simplified medium-voltage network from the United Kingdom Generic Distribution System (UKGDS).

A. UK Generic Distribution System

The 33 kV radial network has 16-buses and is supplied by two identical 33 MVA 132/33 kV transformers with OLTC. The network is illustrated in Fig. 4 [20]. A VR transformer and a sub-sea cable are connecting bus 9 to bus 8. The network supplies a peak load of 38.94 MVA with power factor 0.98 [20]. Half-hourly load profiles, DG generation profiles, and full

network data were obtained from [20]. Based on the load profiles, the network minimum load is 4.74 MVA with power factor 0.98. The network voltage is required to be maintained within ± 6% of the nominal value in accordance with the BS EN50160 standard [15]. In this study, a 3% of the energy demand in the distribution network was considered as the electric vehicles charging loads. Electric vehicles loads were assumed to be distributed in proportion to the peak load at each load bus. An electric vehicle charging profile was obtained from [8].

In the GB power system, DG connection to the distribution network has to comply with engineering recommendation P2/6 [22] to ensure the security of supply. Therefore, the total capacity of DG connected to a distribution network is required not to exceed a level that allows the connection of all DG at rated output under minimum load condition during an outage of the highest rated distribution circuit (which is often the transformer). This is known as the Firm Connection (FC) for generating plants. Accordingly, the UKGDS firm connection is limited to 37.74 MVA (i.e. 33 MVA transformer capacity plus 4.74 MVA minimum load).

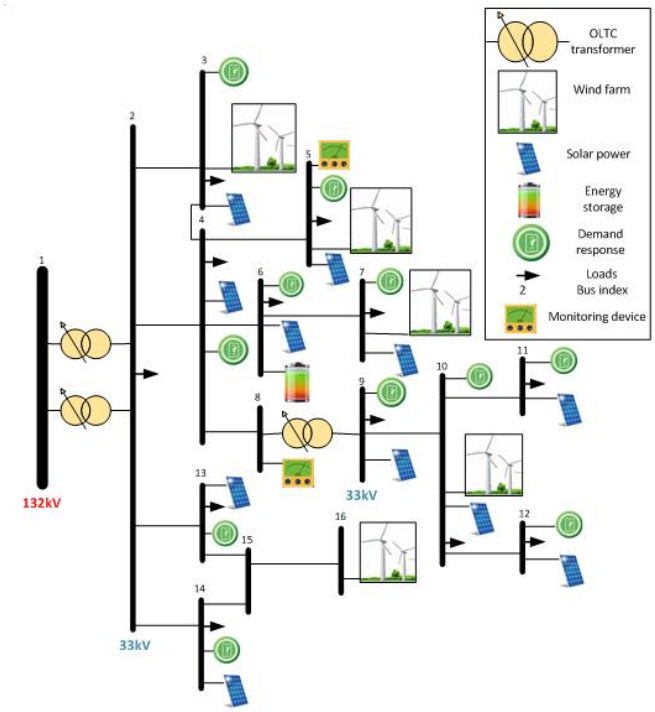

Fig 4. UK generic distribution system used

B. DG Allocations

Two types of DG were considered in this study. The first type is the domestic photovoltaic (PV). PVs were connected to 11 buses were assumed to be distributed in proportion to the peak load at each bus. The PV penetration level at each bus ($PV\%_i$) is set according to (13).

$$PV\%_i = \frac{P^{rated}{}_{PV\_i}}{Pl^{\max}{}_i} \tag{13}$$

where $P^{rated}{}_{PV\_i}$ is the aggregated rated power of all PVs connected to bus i and $Pl^{max}{}_i$ is the max. total load of bus i.

The second type of DG is wind-farms. In addition to the existing wind-farm at bus 16, four extra wind-farm locations were considered (Fig. 4). All wind-farms were located far from the substation and at the end of individual feeders.

The network hosting capacity, defined as the total DG capacity under the minimum loading condition, was obtained by Genetic Algorithm (GA). Genetic Algorithm maximises the total wind-farms capacity at a given PV penetration level. Genetic Algorithm iteratively modifies a population of individual solutions. For each GA solution, MATPOWER [22] was employed to find load flow solution to check voltage and thermal limits constraints. Under 20% PV penetration level (i.e. 6.55 MW), 41.9 MW of wind-farms capacity was allowed into the network. Hence, the network hosting capacity is 48.45 MW.

C. VESS Allocation

All the network load buses (12-buses in total), were assumed to have flexible loads except the main bus (i.e. bus no. 2). The demand response penetration level at each bus ($DR\%_i$) is defined in (14)

$$DR\%_i = \frac{Pl^{\max}{}_{DR\_i}}{Pl^{\max}{}_i} \tag{14}$$

where $Pl^{max}{}_{DR\_i}$ is the aggregated max. power of all demand response units connected to bus i and $Pl^{max}{}_i$ is the max. total load of bus i.

In this paper, bitumen tank was used to demonstrate demand response capabilities. Under 30% demand response penetration level, 9.8 MW of demand response aggregated capacity was connected to the distribution network. Assuming all bitumen tanks have a typical power consumption of 40 kW, 245 bitumen tanks are connected in the distribution network.

In the presence of flexible loads (i.e. demand response units), the distribution network hosting capacity for DG is increased. The hosting capacity for DG with demand response was obtained by GA. That is, with 9.8 MW of demand response aggregated capacity, 60.25 MW of DG allowed into the network. This 60.25 MW DG capacity is composed of, 20% PV penetration level (i.e. 6.55 MW) and 53.70 MW of wind-farms capacity.

Fig. 5 shows the effect of different DG penetration levels (i.e. 0%-200% of the UKGDS hosting capacity for DG) on the UKGDS network maximum voltage deviation considering the cases with and without the voltage control scheme of the VESS. The 100% DG penetration level indicates the UKGDS hosting capacity for DG of 60.25 MW. Under low DG penetration levels (i.e. less than 60%), the maximum voltage deviation in the UKGDS network with and without the control scheme of the VESS were similar. Under high DG penetration levels (i.e. 60% to 100%), the VESS voltage control scheme controlled the maximum voltage deviation to remain within the voltage limit (i.e. 0.06 p.u.) while the maximum voltage deviation exceeded the voltage limit without the VESS voltage control scheme. When the DG penetration level is higher than the network DG hosting capacity (i.e. higher than 100%), the maximum voltage deviation in the UKGDS network with and without the control scheme of the VESS were both breaching the voltage limits. With DG penetration levels higher than 100 % however, the voltage control scheme of the VESS reduced the maximum voltage violation more than the base case. Fig. 5 therefore shows that the voltage control scheme of the VESS is able to reduce voltage violations caused by DG penetration levels

higher than the UKGDS network hosting capacity (i.e. 100% or 60.25 MW).

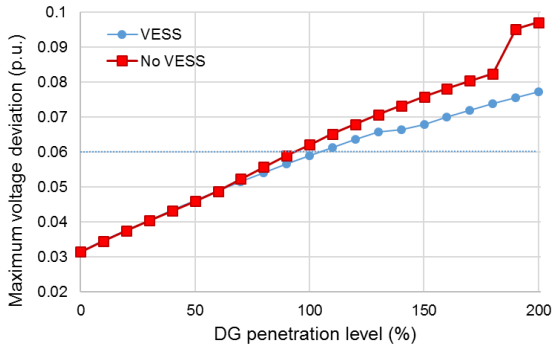

Fig.5. UKGDS maximum voltage deviations at different DG penetration levels.

The energy storage system is utilised to compensate for the demand response uncertainty. Its location was decided by voltage sensitivity factors. Hence, the energy storage system is connected to the bus having largest values of voltage sensitivity factors with respect to the monitored buses. The monitored buses are the most vulnerable buses with respect to voltage violation. By analysing the UKGDS, bus 5 (with the largest load) and bus 8 (which connects VR with several buses) were nominated to be monitored by the energy storage system controller. To validate selecting these buses, for the DG capacity of 60.25 MW and less DR penetration level (20% rather than 30%), buses 5,7, and 8 had voltage violation problems. Bus 6 had the largest voltage sensitivity factors with respect to buses 5,7, and 8, therefore energy storage system was connected to bus 6. Power and energy capacities of the energy storage system were determined through running time series power flow of the distribution network with DG at different periods of the year and checking for voltage violations. Whenever a voltage violation occurs, the required energy storage system active and reactive powers were calculated to eliminate that violation according to (12). As a result, the energy storage system power capacity was the maximum value of the calculated active power whereas its energy capacity was the integration of consecutive active power deployed/absorbed. For 9.83 MW capacity of demand response and 60.25 MW capacity of DG and through one summer week, one winter week and one spring day periods, the energy storage system rated power and energy capacities were calculated to be 2.3 MW and 1.4 MWh. The maximum reactive power was limited to 0.8 times of the rated active power similar to the energy storage system installed in the CLNR project [5] to reduce the size of the converter installed.

VI. Case Study

In this section the performance of VESS coordinated control was assessed against a base case with no VESS and the DG capacity was 60.25 MW.

In the base case, the UKGDS network voltage was only controlled by OLTC and VR transformers. The controllers of OLTC and VR discretely change the transformer tap position to regulate the transformer secondary voltage with a corresponding set-point and a bandwidth. Both OLTC and VR have 20 tap positions (-0.85 +0.05 as a per unit nominal value). When the voltage diverts outside the bandwidth for a time longer than the controller time constraints (τ_{OLTC} and τ_{VR}), the controller takes actions to return the voltage to the set-point by changing the transformer tap position in proportion to the voltage diversion.

One voltage set-point for VR and two voltage set-points for OLTC were determined, i.e. a high-load winter set-point and a low-load summer set-point (Table II). To determine OLTC and VR set-points, one winter week and one summer week load profiles (without DG) were used to adjust the set-points so that no voltage violation will take place in the distribution network.

TABLE II
OLTC AND VR CONTROLLER SETTINGS

	Parameter	Value (p.u.)
OLTC	Voltage set-point/winter	1.0265
	Voltage set-point /summer	1.02
	Bandwidth	0.011
VR	Voltage set-point /all year	1.02
	Bandwidth	0.013

Power flow analysis with 1-min resolution was carried out using MATPOWER. Bitumen Tanks and battery energy storage system models, and OLTC and VR controllers were all implemented using MATLAB. To evaluate the proposed VESS control scheme performance over different seasons of the year, the following three periods were investigated. Results were compared with the base case in which no VESS was used.

Case One: A spring day with high DG power output and low network demand.

Case Two: A winter week with high wind energy generation.

Case Three: A summer week with high solar generation.

Case Four: An autumn week with high wind and solar generations and a medium demand.

Due to page limit, the results of Case One will be presented in detail and results of the other two cases will be summarised in a table.

Fig. 6 shows the total load, wind and solar generations as a base case without VESS. In this case a coincidence of high DG output and low load led to voltage violation in the first five hours of the day (see Fig. 7).

The VESS and its control scheme in section IV were employed to control the network voltage. ESS monitors buses 5 and 8 voltages combined with its connected bus 6 and it utilises the voltage sensitivity factors values shown in Table III.

TABLE III
VOLTAGE SENSITIVITY FACTORS (VLOTAGE P.U./POWER P.U.)

	Bus 5 Voltage	Bus 6 Voltage	Bus 8 voltage
ESS Active Power	0.0805	0.564	0.0806
ESS Reactive Power	-0.325	-0.681	-0.326

VESS coordination control scheme accounts for OLTC and VR controllers to eliminate any chance for controller conflicts or voltage hunting among them. The time delay constraints for VESS elements and network transformers are specified in Table IV.

TABLE IV
VESS AND TRANSFORMERS CONTROL TIME DELAY

Parameter	Time Delay (min.)
τ_{DR}	1
τ_{ESS}	2
τ_{VR}	3
τ_{OLTC}	4

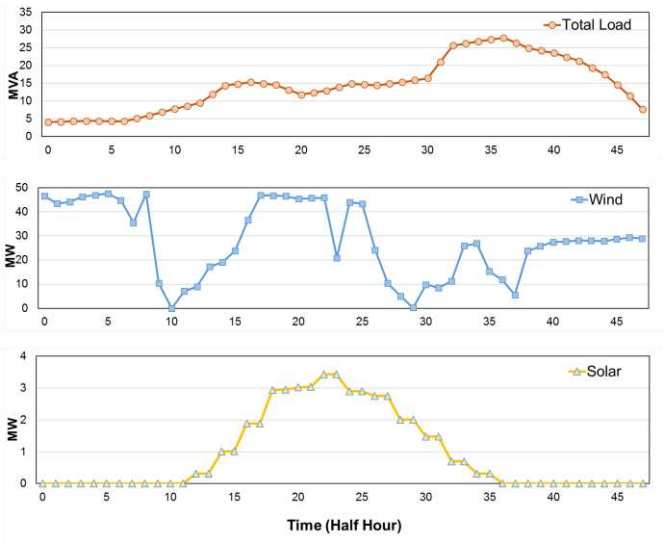

Fig. 6. Load, wind and solar generations for one spring day (case one).

Fig. 8 shows the bus voltages with the proposed VESS. The network complies with BS EN50160 and all bus voltages are within limits. Moreover, the proposed VESS control scheme reduces the network OLTC and VR transformers actions in all cases except number of VR tap changes in summer (Table V) and hence reduces their maintenance requirements and prolongs their life. The number of tap changes of the VR transformer with the voltage control scheme of the VESS increased slightly during the summer week compared with the base case, due to the increase in voltage variations with the voltage control scheme. An equivalent capacity of loads (i.e. 30% of the total load) in the base case was replaced by bitumen tanks for demand response in the VESS. Therefore, the response of bitumen tanks combined with the low demand (i.e. summer week demand) from the remaining loads (i.e. non-flexible loads) led to a higher total load variation than the base case. This higher total load variation triggered slightly different voltage variations than the base case, which caused he slightly more numbers of tap changing actions.

Fig. 10 shows the distribution of buses voltages over the spring day. The number of samples is 720 (i.e. 15 buses over 48 time intervals). Fig. 10 shows that with the VESS voltage control scheme, the voltage violations were eliminated and all buses with very high voltages were reduced to the voltage permissible limit (i.e. 1.06 p.u.). Other cases also showed similar results. With the VESS voltage control scheme, the number of buses with permissible high voltages was increased (i.e. between 1.03-1.06 p.u.). However, the ability of UKGDS network to host a greater DG generation capacity (i.e. 48.45 MW without the VESS to 60.25 MW with the VESS) was not affected since all buses voltages were controlled to remain within the limits.

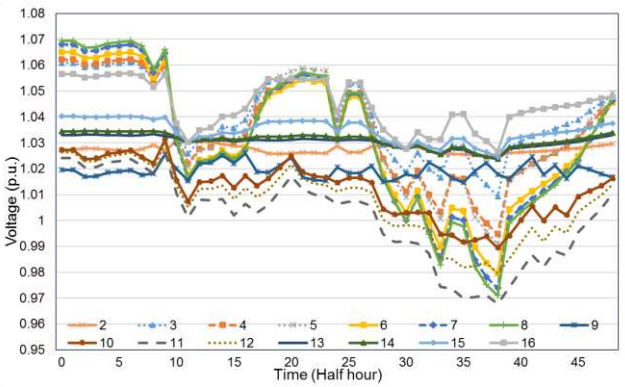

Fig. 7. Distribution network bus voltages without VESS for one spring day (case one).

TABLE V
VESS CONTROL PERFORMANCE ANALYSIS

Test period	Performance Indicator	No VESS	With VESS
Spring Day Case One	No. of voltage violation buses	44	0
	No. of VR tap changes	32	21
	No. of OLTC tap changes	0	0
Winter Week Case Two	No. of voltage violation buss	7	0
	No. of VR tap changes	191	162
	No. of OLTC tap changes	4	0
Summer Week Case Three	No. of voltage violation buss	2	0
	No. of VR tap changes	79	83
	No. of OLTC tap changes	0	0
Autumn week Case Four	No. of voltage violation buses	2	0
	No. of VR tap changes	101	72
	No. of OLTC tap changes	0	0

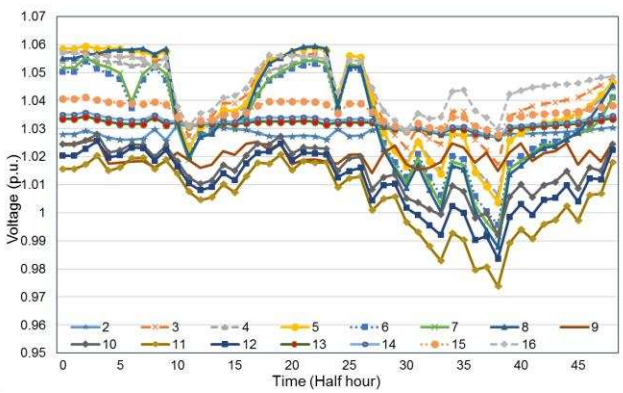

Fig. 8. Voltage of each bus with the VESS for one spring day (case one).

Results in Fig. 11 show that most of the time energy storage system reactive power was sufficient to counteract over-voltage caused by high DG following the limited demand response in case one. The other two cases showed similar behaviour. Limited demand response is a result of reaching their temperature limits and hence needs to be switched on/off to guarantee the temperature performance of Bitumen Tanks.

In addition, it is noted that VESS can prevent the distribution network reinforcements of a third 33MVA transformer and feeder. With the VESS, the maximum power flow through the substation (37.6 MVA) was less than the network FC capacity of 37.7 MVA. Whereas in the base case without VESS, the power flow exceeds (41.9 MVA) the network FC as shown in Fig. 12.

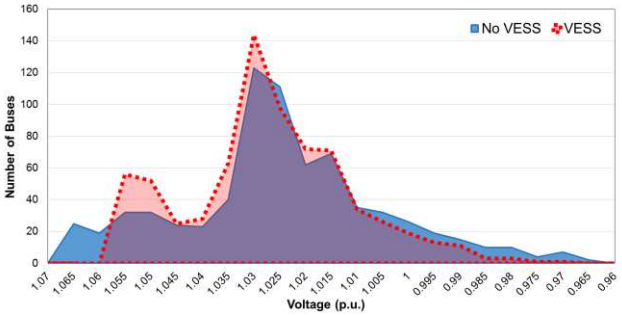

Fig. 10. The distribution of the UKGDS bus voltages for one spring day (case one).

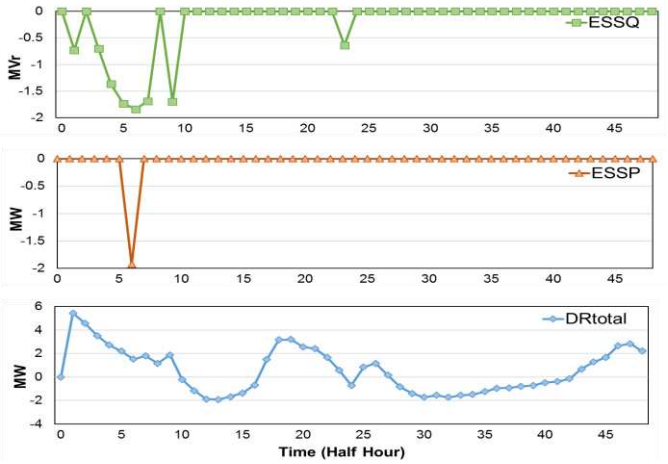

Fig. 11. Response from different VESS elements for one spring day (case one).

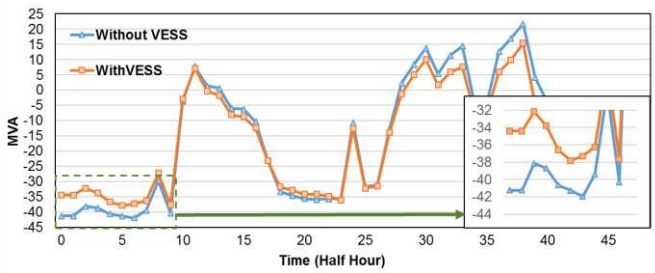

Fig. 12. Power flow through the substation in the UKGDS with and without the VESS for one spring day (case one).

VII. Conclusion

This paper introduces a VESS to provide voltage control in a distribution network which facilitates the integration of DG in the future power system. The VESS consists of flexible loads and an energy storage system. Voltage control of each element in the VESS was developed and coordinated in order to minimise voltage deviations in the distribution network.

The local voltage control of Bitumen Tanks alters the power consumption of flexible loads in response to voltage deviations at the connected bus. The proposed distributed voltage control of Bitumen Tanks has little impact on the primary function of the loads. After the response of flexible loads, the energy storage system local voltage controller monitors the two most vulnerable bus voltages and then determines the charging/discharging actions using the droop control with a droop setting obtained from voltage sensitivity factors. The energy storage system voltage control ensures a firm and linear response from the VESS against voltage violations. In addition, the VESS control scheme coordinates its components and the network inherent voltage control equipment through the setting of time delays to avoid the voltage hunting with a minimum ICT required.

PVs, wind-farms and the VESS were optimally connected to the UKGDS distributed network. Case studies were undertaken to test the performance of the voltage control scheme of the VESS in coordination with the controller of OLTC and VR transformers under different scenarios of DG outputs. The results show that the VESS control scheme eliminates all voltage violations and reduces the required number of OLTC and VR actions, and consequently extends transformer life. The proposed VESS represent an economic and technical alternative to substation upgrade in order to cap with the DG integration in the distribution network.

Acknowledgment

S. S. Sami would like to thank Marc Cheah and Chao Long from Cardiff University for their interesting comments and discussion.

Reference

[1] "System operability framework,", National Grid, UK, 2016.

[2] ElectraLink (2016,October 19) "40% of total renewable output no longer 'invisible' with launch of new energy data analytics service", Available: https://www.electralink.co.uk/2016/10/40-total-renewable-output-no-longer-invisible-launch-new-energy-data-analytics-service-electralink/ .

[3] N. Mahmud and A. Zahedi, "Review of control strategies for voltage regulation of the smart distribution network with high penetration of renewable distributed generation," Renewable and Sustainable Energy Reviews, vol. 64, pp. 582-595, 2016.

[4] "Smarter Network Storage - business model consultation," UK power networks, UK, 2013.

[5] P. Wang, D. H. Liang, J. Yi, P. F. Lyons, P. J. Davison, and P. C. Taylor, "Integrating electrical energy storage into coordinated voltage control schemes for distribution networks," IEEE Transactions on Smart Grid, vol. 5, pp. 1018-1032, 2014.

[6] L. Wang, D. H. Liang, A. F. Crossland, P. C. Taylor, D. Jones, and N. S. Wade, "Coordination of multiple energy storage units in a low-voltage dstribution network," IEEE Transactions on Smart Grid, vol. 6, pp. 2906-2918, 2015.

[7] G. Strbac, M. Aunedi, D. Pudjianto, P. Djapic, F. Teng, A. Sturt, et al., "Strategic assessment of the role and value of energy storage systems in the UK low carbon energy future," Report for the Carbon Trust, Energy Futures Lab, Imperial College EDF UK R&D Centre, p. 9, UK, 2012.

[8] "Future Energy Scenarios. GB gas and electricity transmission,", National Grid, UK, 2016.

[9] M. Behrangrad, "A review of demand side management business models in the electricity market," Renewable and Sustainable Energy Reviews, vol. 47, pp. 270-283, 2015.

[10] A. Zakariazadeh, O. Homaee, S. Jadid, and P. Siano, "A new approach for real time voltage control using demand response in an automated distribution system," Applied Energy, vol. 117, pp. 157-166, 2014.

[11] E. Vrettos, K. Lai, F. Oldewurtel, and G. Andersson, "Predictive Control of buildings for Demand Response with dynamic day-ahead and real-time prices," in *2013 European Control Conference (ECC)*, 2013, pp. 2527-2534.

[12] S. A. Pourmousavi, M. H. Nehrir, and R. K. Sharma, "Multi-Timescale Power Management for Islanded Microgrids Including Storage and Demand Response," *IEEE Transactions on Smart Grid,* vol. 6, pp. 1185-1195, 2015.

[13] D. Wang, S. Ge, H. Jia, C. Wang, Y. Zhou, N. Lu, et al., "A demand response and battery storage coordination algorithm for providing microgrid tie-line smoothing services," IEEE Transactions on Sustainable Energy, vol. 5, pp. 476-486, 2014.

[14] M. Cheng, S. S. Sami, and J. Wu, "Benefits of using virtual energy storage system for power system frequency response," Applied Energy, 2016.

[15] M. Cheng, J. Wu, S. J. Galsworthy, C. E. Ugalde-Loo, N. Gargov, W. W. Hung, et al., "Power System Frequency Response From the Control of Bitumen Tanks," IEEE Transactions on Power Systems, vol. 31, pp. 1769-1778, 2016.
[16] M. Cheng, "Dynamic demand for frequency response services in the great britain power system," PhD thesis, Cardiff University, Cardiff, UK, 2014.
[17] S. S. Sami, C. Meng, and J. Wu, "Modelling and control of multi-type grid-scale energy storage for power system frequency response," in 2016 IEEE 8th International Power Electronics and Motion Control Conference (IPEMC-ECCE Asia), 2016, pp. 269-273.
[18] "Voltage characteristics of electricity supplied by public distribution networks,", British Standard EN 50160, 2007.
[19] Y. He, M. Petit, and P. Dessante, "Optimization of the steady voltage profile in distribution systems by coordinating the controls of distributed generations," in 2012 3rd IEEE PES Innovative Smart Grid Technologies Europe (ISGT Europe), 2012, pp. 1-7.
[20] " United Kingdom Generic Distribution System (UKGDS)", Distributed Generation and Sustainable Electrical Energy Centre, [Online]. Available: http://www.sedg.ac.uk/
[21] "Engineering Recommendation P2/6,", Energy Networks Association, UK, 2006.
[22] R. D. Zimmerman, C. E. Murillo-Sanchez, and R. J. Thomas, "MATPOWER: Steady-State Operations, Planning, and Analysis Tools for Power Systems Research and Education," IEEE Transactions on Power Systems, vol. 26, pp. 12-19, 2011.

Saif S Sami (S'14) received his BSc and MSc from Baghdad University in 2004 and 2008 respectively. Currently, he is a final year PhD student in the School of Engineering, Cardiff University, Cardiff, U.K. His research interests include energy storage systems and demand response.

Meng Cheng received the B.Sc. degrees in electrical and electronic engineering from Cardiff University, U.K. and North China Electric Power University (Beijing), China, in 2011, and the Ph.D. degree from Cardiff University in 2015. She is currently a Research Associate with Cardiff University. Her research interests include smart grids and dynamic demand.

Jianzhong Wu (M'06) received the Ph.D. degree in electrical engineering from Tianjin University, Tianjin, China, in 2004. He is currently a Professor with the Institute of Energy, Cardiff University, Cardiff, U.K. His research focuses on energy infrastructure and smart grid.

Nick Jenkins (M'81–SM'97–F'05) received the B.Sc. degree from Southampton University, Southampton, U.K., in 1974, the M.Sc. degree from Reading University, Reading, U.K., in 1975, and the Ph.D. degree from Imperial College London, London, U.K., in 1986. He is currently a Professor and Director, Institute of Energy, Cardiff University, Cardiff, U.K. Before moving to academia, his career included 14 years of industrial experience, of which five years were in developing countries. While at university, he has developed teaching and research activities in both electrical power engineering and renewable energy.